



INTEGRATING COMPUTATIONAL METHOD FOR DRUGGABLE BETA CATENIN INHIBITORY PHYTOCOMPOUND FROM *GLYCINE MAX L. SEEDS TO TREAT OVARIAN CANCER*

Samra Hafeez¹, Asma Ahmed^{2*}, Maryam Mureed³, Hamna shahid⁴, Afaq Akram⁵

^{1,2*,3,4,5}Institute of Molecular Biology and Biotechnology, The University of Lahore, Lahore,
Punjab, Islamic Republic of Pakistan

***Corresponding Author:** Asma Ahmed

*Institute of Molecular Biology and Biotechnology, The University of Lahore, Lahore, Punjab,
Islamic Republic of Pakistan, E-mail: asma.ahmed@imbb.uol.edu.pk

Abstract

Ovarian Cancer is the most lethal gynecological malignancy and is ranked as the seventh leading cause of cancer deaths in females. Wnt signaling is an evolutionarily conserved regulatory pathway that governs numerous normal cellular and developmental processes such as cell fate determination, cell proliferation and migration. However, aberrant Wnt signaling has also been identified as a key mechanism in cancer biology. β -catenin is the key mediator of the Canonical Wnt pathway. In the absence of a Wnt ligand, β -catenin is degraded by a destruction complex. The main components of this complex include AXIN, adenomatous polyposis coli (APC), casein kinase 1 (CK1), and glycogen synthase kinase 3 β (GSK3 β), as well as the E3 ligase, β TrCP. Protein phosphatase 2A (PP2A) is also associated with the β -catenin destruction complex. AXIN is a scaffolding protein that has interaction sites for multiple proteins including PP2A, APC, GSK3 β , and CK1. The most common genetic alteration in the Wnt/ β -catenin pathway involved in EOC is in the β -catenin gene, CTNNB1. In EOCs a missense mutation in CTNNB1 was always found within the amino terminal domain. Soybeans (*Glycine max L.*), a functional food widely consumed in Asia, has been reported as the main source of isoflavones. Phytoestrogen properties of soy isoflavones showed their activity as ligands for estrogen receptors and exhibited the estrogenic potency as reported in the previous in vitro and in vivo studies. The major functional components include Carbohydrates, fats, Proteins, Saponins, Lecithin, Linolenic acid, Linoleic acid, Phytosterols and Isoflavones. Due to these valuable constituents, it possesses multiple therapeutic activities. Current *in-silico* study showed that Daidzein from *G. max L.* has maximum binding affinity with beta catenin, which may be ultimately inhibited followed by the inactivation of Wnt/ β -Catenin pathway. Moreover, it has been shown to relieve sleep disorders, may help managing diabetes, prevents osteoporosis, improves blood circulation and provide good care of pregnancy.

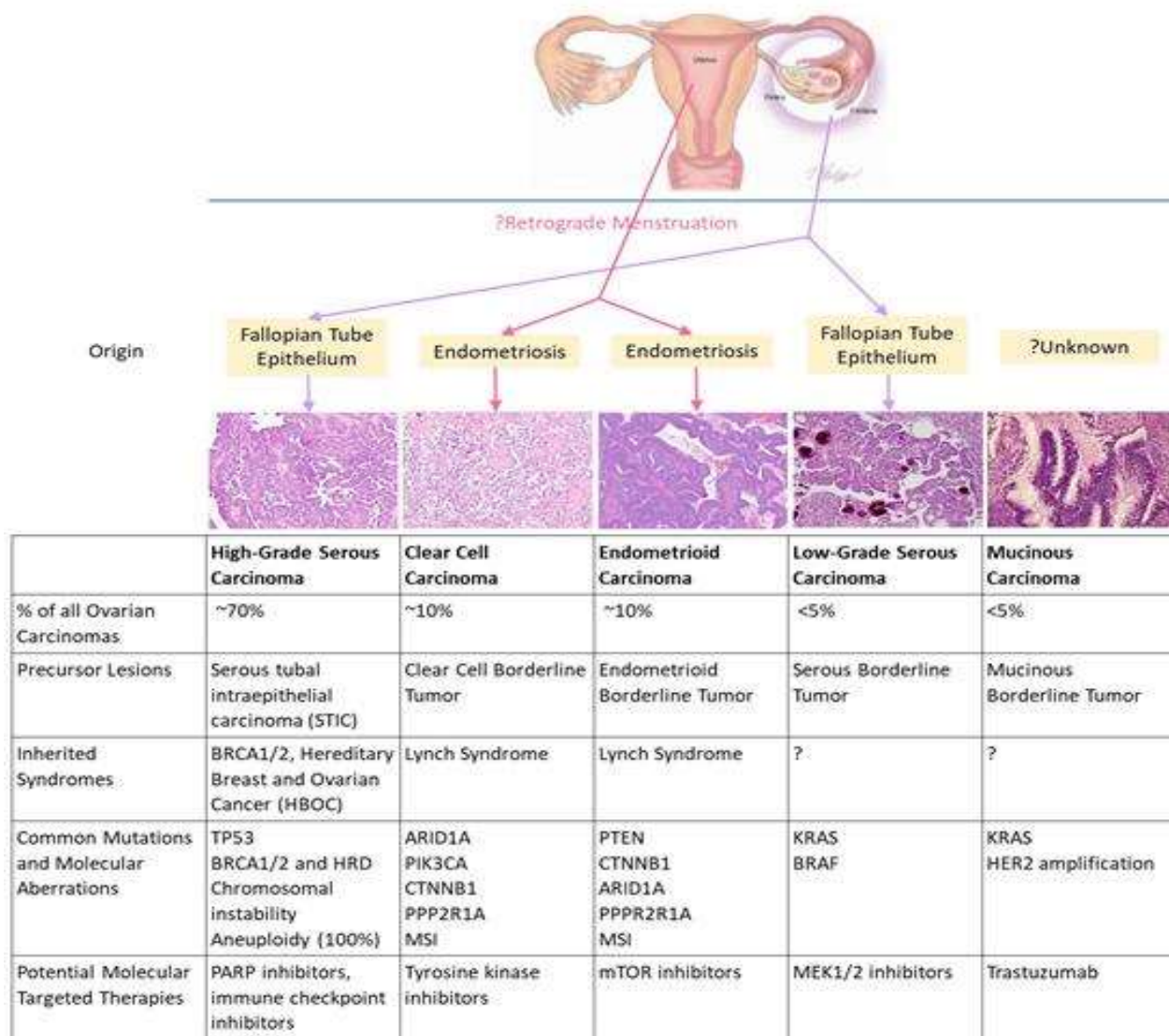
Keywords: Ovarian Cancer, Wnt/ β -catenin inhibition, Phytocompound, *Glycine max L.*

INTRODUCTION

According to the estimates by The American Cancer Society regarding incidence of ovarian cancer in the United States for 2023 about 19,710 women will receive a new diagnosis of ovarian cancer and about 13,270 women will die from ovarian cancer. The deadliest among gynecologic malignancies

Epithelial ovarian cancer (EOC) is ranked as the 5th leading cause of cancer deaths in females (Siegel RL, Miller KD, Jemal A (2019) accounting for more deaths than any other cancer of the female reproductive system. Ovarian cancer stages range from stage I (1) through IV (4). As a rule, the lower the number, the less the cancer has spread. A higher number, such as stage IV, means cancer has spread more (1). The most commonly adopted **ovarian cancer staging** system is the FIGO staging system. On the basis of its cellular origins, clinical characteristics, morphological findings, and several other molecular epigenetic/ genetic alterations, epithelial ovarian cancer (EOC) has been subdivided into five main types (Table 1) (2, 3).

Table 1 Major types of EOC



As noted, EOC is found to be an extremely heterogeneous disease. Multiple genetic/ epigenetic alterations are observed at a broad spectrum of oncogenes and tumor suppressor genes leading to deregulation and aberrant activity of signal transduction pathways whose functions ranges from cell proliferation, cell adhesion, DNA repair, apoptosis and motility (4). Type I lesions frequently carry mutations in KRAS, BRAF, PTEN, and CTNNB1 (β -catenin), and often show a relatively stable karyotype (5,6). Type II ovarian cancers include undifferentiated carcinomas and high-grade serous (HGS). The vast majority of which characterized by TP53 alterations and pronounced genomic instability (7). Inherited and somatic BRCA1 and BRCA2 mutations are commonly found in type II tumors (8).

1. Genetic alteration of the Wnt/ β -catenin pathway in ovarian cancer

The most common genetic alteration in the Wnt/ β -catenin pathway involved in EOC is in the β -catenin gene, CTNNB1 [21]. Mutations in this gene often result in an increased nuclear accumulation of β -catenin and, subsequently, an increase in transcription of its target genes [30] (Figure 1). The Wnt/ β -catenin pathway regulates cell proliferation, polarity, survival, and stem cell fate in embryonic and adult tissue *homeostasis* (9, 10). The proper activity of this pathway is tightly regulated. It is well documented now that aberrant Wnt signaling or any deregulation is associated with the development of so many pathologies, including cancer (11) (Figure 2).

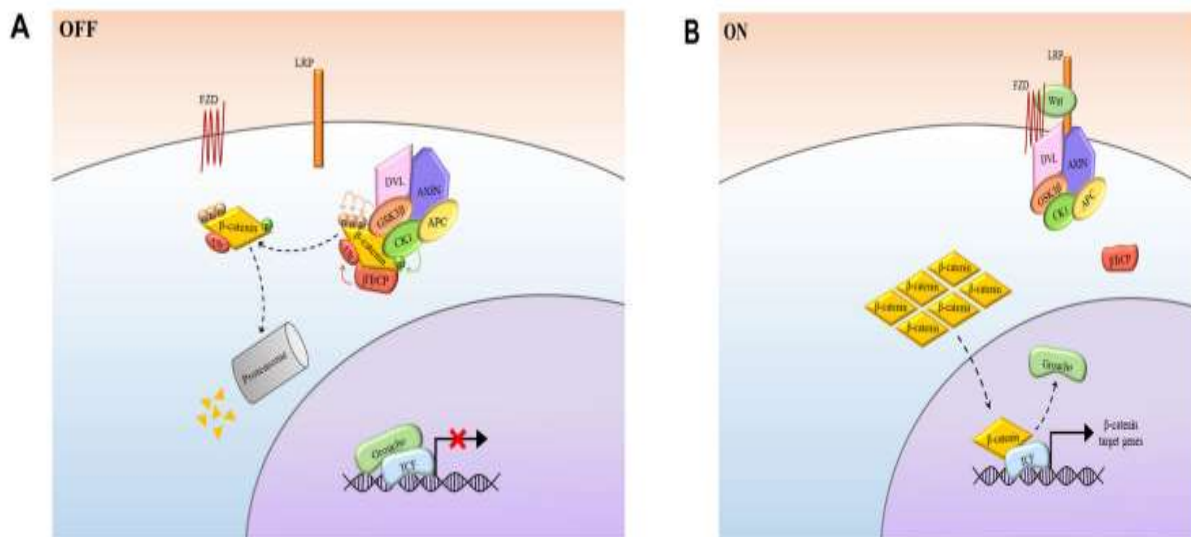


Figure 1 The Wnt/ β -catenin signaling pathway. (A) Wnt signaling OFF. (B) Wnt signaling ON.

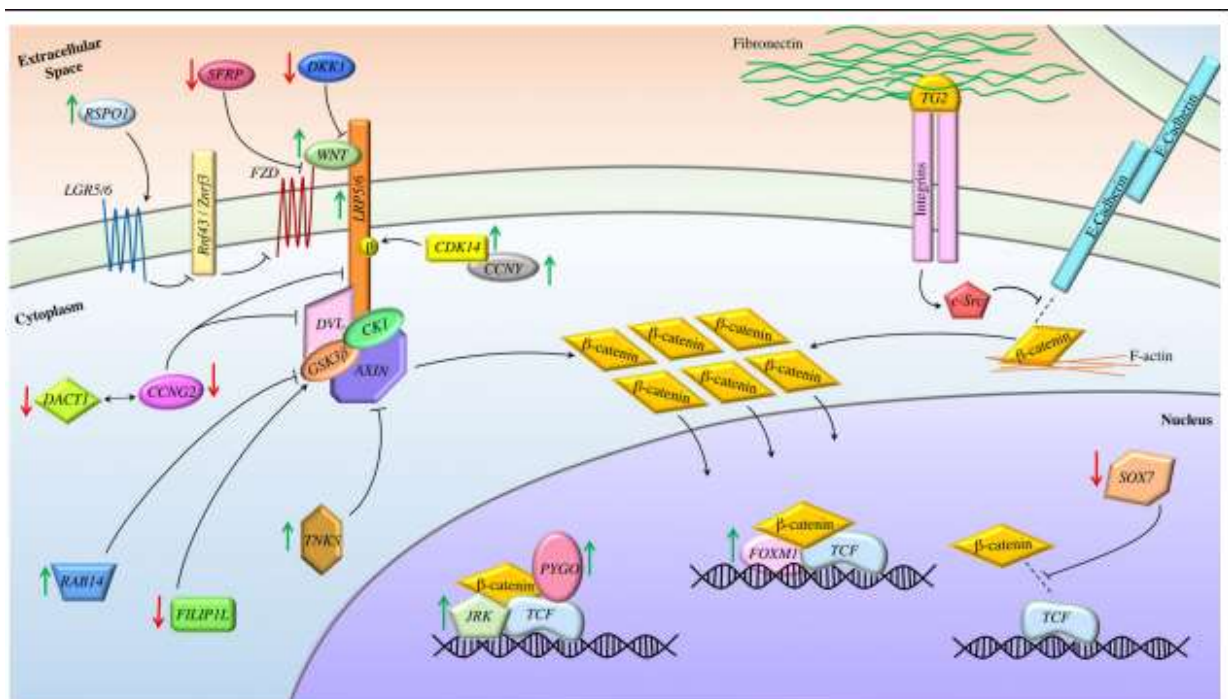


Figure 2 Proposed mechanisms of Wnt/ β -catenin dysregulation in ovarian cancer

Green arrows indicate proteins whose expression is upregulated in EOC, while red arrows indicate downregulation. DKK1 and SFRP2 inhibit the dimerization of FZD and LRP5/6 and directly prevent FZD activation, respectively, are downregulated in EOC tumors. In contrast, Wnt ligands activate the pathway by forming a receptor complex with FZD and LRP5/6, while R-spondins bind LGRs and

prevent the sequestration of the FZD. Both ligands and LGRs are overexpressed EOC. CCNY and CDK14 are also upregulated in EOC and have been suggested to work together to promote LRP5/6 phosphorylation and therefore activation. CCNG2, which is downregulated in EOC, decreases LRP6 and DVL levels. It may also interact with DACT1, also downregulated in EOC tumors, to promote DVL degradation. TNKS destabilizes AXIN to increase β -catenin activity and TNKS1 is known to be up-regulated in EOC. RAB14 inhibits the activity of GSK-3 β and its upregulation contributes to higher β -catenin activity in EOC. FLIP1L, whose expression is negatively correlated with EOC progression, enhances GSK-3 β activation in the destruction complex and is downregulated in EOC. This inhibition of the destruction complex results in the accumulation of β -catenin within the cytosol and its translocation into the nucleus. In addition, TG2, which is overexpressed in EOC, binds to integrin and fibronectin. This results in the recruitment of c-Src and disruption of E-cadherin/ β -catenin complex on the membrane, which contributes to the accumulation of β -catenin within the cytoplasm. Finally, within the nucleus, higher expression of several co-activators of β -catenin/TCF, such as PYGO, JRK, and FOXM1, and lower expression of SOX7, which is known to inhibit the interaction between β -catenin and TCF, lead to the higher transcriptional activity of this complex (Naeema et al. , 2021).

2. Phytochemicals and Epithelial Ovarian Cancer

In recent years, a growing number of studies have uncovered a plethora of potential applications for phytochemicals in signaling pathways related to cancer [16]. Bioactive compounds that can inhibit or antagonize factors that are dysregulated in malignant cells have the potential to enhance the effects of conventional therapy or be developed into a stand-alone therapeutic in their own right. One major advantage for the use of phytochemicals over synthetic compounds, in many cases, is their historical presence in the human diet. Due to this evolutionary exposure, severe adverse events are conceivably less likely to arise in therapeutic settings when compared to synthetic compounds that are entering the human body for the first time. Modern high-throughput screening techniques can also facilitate the screening of fractionated separations of plant extracts containing thousands of phytochemicals, while synthetic libraries require each candidate to be engineered separately. Some phytochemicals (Table 2) also exert influences on multiple targets within a common oncogenic signaling pathway [17]. Many oncogenic signaling pathways are shared by malignant cells across different tissue types, due to common functional requirements for sustained survival and proliferation. Therefore, phytochemicals that exhibit anticancer activity in one cell type may have potential for application in treating a wider range of cancers (18).

Table 2 Phytochemicals with their rich sources in food

Categories of Phytochemicals	Sub-categories of phytochemicals	Compounds	Food source	Citations
Polyphenols	Flavonoids	Quercetin, Kaempferol	Onions, leeks, broccoli, buckwheat, red grapes Tea and apples	Rehman et al. , 2023
	Flavan-3-ols (Tannins):	Catechins, Epicatechins, Epigallocatechin gallate	Tea, chocolate and grapes	Gul et al. , 2022
	Dihydrochalcones	Phloridzin, Aspalathin	Apples and rooibos tea	Shinwari et al. , 2022
	Flavanolols	Silymarin, Silibinin, Aromadredrin	Milk thistle and red onions	Asma et al. , 2023
	Flavones	Apigenin, Luteolin	Celery, herbs, parsley, chamomile, rooibos tea, Capsicum and pepper	Naeema et al. , 2021
	Isoflavones	Genistein, Daidzein, Glycitein	Soya, beans, chickpeas alfalfa and peanuts	Asma et al. , 2023, Ghazala et al. , 2023
	Flavanones	Naringenin, Hesperidin	Citrus fruit	Zhang et al. , 2018
	Anthocyanidin		Red grapes, blueberries, cherries, strawberries, blackberries and Raspberries and tea	Naeema et al. , 2021; Asma et al. , 2021

Integrating Computational Method For Druggable Beta Catenin Inhibitory Phytochemical From *Glycine Max* L. Seeds To Treat Ovarian Cancer

Phenolic Acids	Hydrobenzoic acid	Gallic acid	Rhubarb, grape seed, raspberries, blackberries, pomegranate Vanilla and tea	Farah et al. , 2023; Ghazala et al. , 2023
		Ellagic acid	<i>Pinus roxburgii</i> , onion, tea, garlic	Hasan et al. , 2023
		Vanillic acid	Cereals, fruits, flaxseed, Sweet potato	Hasan et al. , 2023
	Hydroxycinnamic acid	Ferulic acid	Wheat bran , cinnamon, coffee, kiwi fruit , plums , blueberries	Hasan et al. , 2023; Asma et al. , 2023, Ghazala et al. , 2023
		P-coumaric acid	peanuts, navy beans, tomatoes, carrots, basil and garlic	Ferreira et al. , 2019
		Caffeic acid	Tea, Coffee	Hasan et al. , 2023; Asma et al. , 2023, Ghazala et al. , 2023
	Sinapic acid	oranges, grapefruits, and cranberries and in herbs like canola, mustard seed and rapeseed.	Pandi et al. , 2021	
Other non - flavonoids polyphenols	Tannins	Tannic acid	Cereals, fruits, berries, beans, nuts. wine, cocoa	Jing et al. , 2018
	Curcuminoids	Curcumin	Turmeric	Pandi et al. , 2021
	Cinnamic acid		Grapes, wine, blueberries, peanuts, raspberries	Hasan et al. , 2023; Asma et al. , 2023, Ghazala et al. , 2023
	Resveratrol		Pistachios, Grapes, Red wine, peanuts, knotweeds, pine trees including Scots pine and Eastern white pine, grape vines, raspberries, mulberries, peanut plants, cocoa bushes, and Vaccinium	Fogacci et al. , 2018
	Lignans	Secoisolariciresinol	Grains, flaxseed, sesame seeds	Asma et al. , 2023, Ghazala et al. , 2023
		enterolactone	Sweet potato, sesame seeds	Pandi et al. , 2021
Sesamin		sesame seeds	Pandi et al. , 2021, Fogacci et al. , 2018	
Terpenoids	Carotenoids	Alpha, beta and gamma Carotene	Sweet potato, carrots, pumpkin, kale	Wu et al. , 2021
		Lutein	Corn, eggs, kale, spinach, red pepper, pumpkin, oranges	Cooney et al. , 2019
		Zeaxanthin	Corn, eggs, kale, spinach, red pepper, pumpkin, oranges	Kim et al. , 2020
		Lycopene	Tomatoes, water- melon, pink grapefruit, guava, papaya	Timlin et al. , 2021
		Astaxanthin	Salmon, shrimps. Krill, crab	Powers et al. , 2021
	Non-carotenoids terpenoids	Saponins	Chickpeas, soybeans	Tatli et al. , 2021
		Limonene	The rind of citrus fruits	Khadija et al. , 2023
		Perillyl Alcohol	Cherries, caraway seeds, mint	Chen et al. , 2015
		Phytosterols	Vegetable oils, cereal grains, nuts, shoots, seeds and their oil, whole grains, legumes	Li et al. , 2022
		Urosolic acid	Apples, cranberries, prunes, peppermint Oregano, thyme	Zhang et al. , 2020; Cargin and Gnoatto. (2017)
		Ginkgolide and bilobalide	<i>Ginkgo biloba</i>	Forman et al. , 2022
Thiols	Glucosinolate	Isothiocyanates (Sulforaphane)	cruciferous vegetables such as broccoli, asparagus, brussel sprouts, cauliflower, horseradish, radish and mustard	Palliyaguru et al. , 2018; Asif et al. , 2023
		Dithiolthiones	raw and fresh vegetables, leafy green vegetables, Cruciferae, carrots, broccoli, cabbage, lettuce, and raw and fresh fruit (including tomatoes and citrus fruit)	Ansari et al. , 2018; Zhang and Munday, 2008
	Allylic sulphide	Allicin	Garlic, leeks, onion	Asma et al. , 2018
		S-allyl cysteine	Garlic	Yudhistira et al. , 2022; Asma et al. , 2018
	Indole-3-carbinol	Broccoli, brussel sprouts	Kundu et al. , 2017	

	non-sulphur containing indols	Betaines	Beetroots	Arumugam et al., 2021
		Chlorophylls	Green leafy vegetables	Yudhistira et al. , 2022; Ansari et al. , 2018; Zhang and Munday, 2008
		Capsaicin	Chilli	Kim et al. , 2020; Cooney et al. , 2019
		Peperine	Black pepper	Kim et al. , 2020; Cooney et al. , 2019

Soybeans (*Glycine max* L.), a functional food widely consumed in Asia, has been reported as the main source of isoflavones. Phytoestrogen properties of soy isoflavones showed their activity as ligands for estrogen receptors and exhibited the estrogenic potency as reported in the previous *in vitro* and *in vivo* studies. Soy foods became most popular due to their benefits to human health and body function. The utilization of chemometrics in soybean isoflavones extraction and authentication was reported along with the increasing trends of computational analytical chemistry.

MATERIALS AND METHODS

1. Selection of ligand

To investigate the potential anticancer properties of glycine max seeds out of 44 ligands 12 were selected namely 2 Pentylfuran, Ascorbic acid, Quercetin, Coumesterol, Daidzein, Formononetin, Genistein, Genistin Isoflavones, Gibberellin A1, Glycitein, Glycitin and N6 Methylagmatine. These ligands were chosen on the basis of their ability to interact with the selected protein beta catenin and were subjected to compound screening for drug development before advancing to costly clinical trials. The ADMET properties of the drug candidates were evaluated through the server of SwissADME (jamkhedkar 2023) to ensure their safety and efficacy which are necessary for regulatory approval. Following the Lipinski's rule of five, which takes into account things like a molecular weight of less than 500, a logP of less than 5, under than five H-bond donors and fewer than ten H-bond acceptors, the selected compounds were evaluated and hence screened present in glycine max seeds and finally selected the best among all following it.

All selected compounds were then docked with receptors using CB dock (Liu et al, 2020). COACH server (Yang et al, 2023) and SPPIDER (Porollo & Miller, 2007) were used to find interacting residues. Docked complexes were then correlated with ligpl (Laskowski & Swindells, 2011) to find actual binding residues of ligand with receptor protein.

2. Preparation of ligand

SDF files of compound from Glycine Max seeds were obtained from the IMPPAT (Indian Medicinal Plant Phytochemistry and Therapeutics) with their respective ID. IMPPAT 2.0 is the largest digital database on phytochemicals of Indian medicinal plants to date which is manually curated database and has been constructed via digitalization of information from more than 100 books on traditional Indian medicine.

3. Target/protein identification

For structure of targeted protein, (beta catenin) FASTA sequences of beta catenin was obtained from UniProt of *Homo sapiens* (the UniProt Consortium 2019) and their 3D structures was obtained from Swiss model (Waterhouse et al 2018). Best model obtained was selected on the basis of GMQE (Global Model Quality Estimation) and QMEAN (Qualitative Model Energy Analysis) and coverage and sequence identity (Waterhouse et al 2018). Model was protonated, tethered, and all the water molecules were removed by using Discovery Studio and Chimera 1.15 (Pettersen et al 2004). Only a single chain of protein was selected on the basis of the homology pattern using Discovery Studio. Then the energy of PDB structure of the receptor was minimized by Yasara and Chiron (Ramachandran et al 2011).

4. Prediction of active sites

Active sites provide required microenvironment for catalysis and allow substrate to form enough contact points for strong binding. If the binding site is identified, docking calculates the binding affinity and stability. To predict the active sites of targeted protein, online tools eF-seek, CB-Dock2 and Coach were used.

5. Molecular docking

Molecular docking analysis was done by PyRx (working on principle of Auto Dock Vina 4) considering the protein as macromolecule and the ligand as phyto-Compounds. All ligands were given as an input. Parameter and protocol were run. The different protein ligand binding patterns were obtained, their binding energy and patterns were analyzed and their 2d and 3d dimensional graphics were also produced.

6. Interaction analysis

Interaction of protein and ligand was analyzed for interacting residues, bond type, bond length and bond distance by Discovery Studio.

7. Post-Trajectory Analysis

CPTRAJ module of AMBER 2.0 was adopted for analysis of hydrogen bond formation and root mean square deviation (RMSD) values acquired after MD simulations (Burmogluet al 2022). Mass weighted RMSD was utilized in the current study and in order to comprehend the extent of deviation of structure from its primary configuration the input coordinate file received following minimization process, was employed as a reference. Hydrogen bond arrangement of 10 complex was evaluated for 10 ns between 80-90ns of trajectories in the trajectory file s(Burmaoglu et al 2022)

8. Binding free energy analysis

MM-GBSA (Molecular Mechanics -Generalized Born Surface Area) and Molecular Mechanics Poisson Boltzmann Surface Area (MM_PBSA) module of AMBER v.20 were employed for computations of binding energies of ligands in complex with acetyl cholinesterase enzyme (Burmaoglu et al 2022). Poisson Boltzmann and generalized Born procedures were adopted for MM_PBSA calculations (igb=5) with salt concentration being 0.15 M. Fill ration of ionic strength values are calculated as 4.0 and 0.15 respectively. Interior dielectric constant was set at default value of 1.0. Evaluation of energy constituents of 10 complex was done for 50ns between 80-90 ns of trajectories. Binding energy has been expressed as $\Delta G_{\text{binding}} = \Delta G_{\text{gas}} + \Delta G_{\text{SOLV}} - TS$ and $\Delta G_{\text{binding}} = \Delta G_{\text{gas}} + \Delta G_{\text{SOLV}}$. Here G_{binding} = Alteration in the free energy of every individual system, EMM = Molecular mechanics energy of the system, ΔG_{gas} = Energy in gaseous phase {internal energy (E_{int}) + van der waals energy (E_{vdw}) + electrostatic energy (E_{elec})}, S = Entropy, ΔG_{Solv} = Molecular mechanics energy [{Total of non-electrostatic free energy of solvation (G_{nonpol}) + dispersion energy (G_{disperse}) + electrostatic energy of solvation (G_{pol}) } at a particularized temperature (T)], TS = Entropic contribution in a vacuum. These energies emanate as a result of dihedral bond and angle interactions. E_{int} determined zero when single trajectory approach was adopted.

9. Molecular dynamics (MD) simulations

MD simulations were performed on the top hits containing high binding energies. Over the simulation period, the projected conformational changes from the initial structure were presented in terms of root mean square deviation (RMSD). Moreover, structural stability, atomic mobility, and residue flexibility at times of interaction of protein-hit were expressed with root mean square fluctuation (RMSF) values. To determine the dynamic binding behavior and binding stability of protein-ligand

complexes in their docked pose, MD simulations were performed using the Desmond. Simulation was run for 100 ns at 1 atm and 300k with NPT ensembles.

RESULTS

1. Evaluation of selected protein structure

Gene encoding for beta catenin was CTNNB1 which downstream component of canonical Wnt signaling pathway and is made up of 781 amino acids (Accession Number is P35222) (Figure 3)

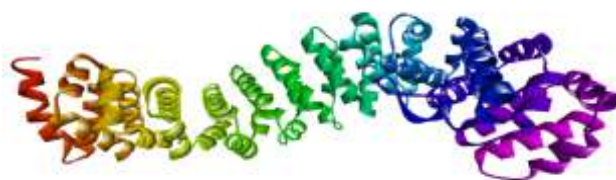


Figure 3 Chemical structure of beta-catenin. Crystal structure of Beta-catenin Armadillo repeats domain in complex with the inhibitor RS6452

There were multiple active binding site residues of three pockets of targeted proteins (Table 2).

Table 2 Active side residues in different pockets of beta catenin

Pocket No.	Active side residues	Servers for prediction
1	E07, D109, S110, L112, F113, K148, N150, K152, F153	eF-seek
2	T53, K254, Q255, E256, G257, M258, N290, N291, K293, N294, M297	CB-Dock2
3	H120, L124, K130, M131, R134, D159, Q162, I163, L164, Y166, N168, E194, K195, W198, T199, R202, K205, V206, R236, 240	

Where: A: Alanine, R: Arginine, N: Asparagine, D: Aspartic acid; C: Cysteine; E: Glutamic acid; Q: Glutamine; G: Glycine; H: Histidine, I: Isoleucine, L: Leucine; K: Lysine; M: Methionine; F: Phenylalanine, P: Proline; S: Serine; T: Threonine; W: Tryptophan, Y: Tyrosine; V: Valine.

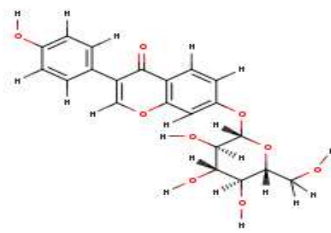
2. Evaluation of different features of selected ligands

Binding affinity, interacting residues, molecular formulas and molecular weight of selected phytochemicals showed a range of variations which have been shown with their IMPPAT ID (Table 3, Figure 4).

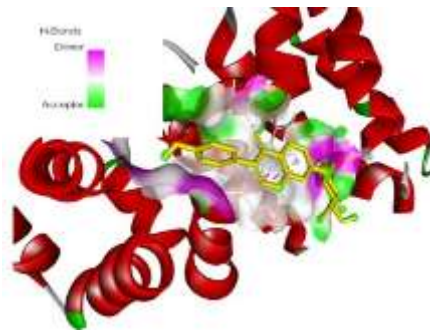
Table 3 Features of selected phytochemicals of *G. max* (Seed)

Phytochemicals	IMPAT ID	Binding Affinity (Kcal/mol) with beta catenin	Interaction residues of beta catenin	Molecular Formula of phytochemical	Molecular weight (g/mol) of phytochemical	Figures 4
2 Pentylfuran	IMPHY005811	-4	Phe113, Try114, Phe153	C ₉ H ₁₄ O	138.21	A (i, ii, iii)
Ascorbic acid	IMPHY006362	-4.5	Lys254, Asn291, Tyr292	C ₆ H ₈ O ₆	176.12	B (i, ii, iii)
Quercetin	IMPHY004619	-6.2	Gln162, Arg202, Lys205, Asn240, Trp243	C ₁₅ H ₁₀ O ₇	302.24	C (i, ii, iii)
Coumesterol	IMPHY004565	-6.8	Arg202, Lys205	C ₁₅ H ₈ O ₅	268.22	D (i, ii, iii)
Daidzein	IMPHY000611	-7.9	Ser110, Phe113, Tyr114	C ₂₁ H ₂₀ O ₉	416.38	E (i, ii, iii)
Formononetin	IMPHY009035	-6.6	Asp109, Ser110, Phe113, Lys148, Phe153	C ₁₆ H ₁₂ O ₄	268.26	F (i, ii, iii)
Genistein	IMPHY004643	-6.5	Tyr166, Arg202, Asn240	C ₁₅ H ₁₀ O ₅	270.24	G (i, ii, iii)
Genistin/soflavones	IMPHY004138	-7.5	Ser110, Phe113, Tyr114	C ₂₁ H ₂₀ O ₁₀	432.38	H (i, ii, iii)
Gibberellin A1	IMPHY004629	-6.4	Arg202, Tyr166	C ₁₉ H ₂₄ O ₆	348.39	I (i, ii, iii)
Glycitein	IMPHY012790	-6.7	Asp109, Ser110, Phe113, Tyr114	C ₁₆ H ₁₂ O ₅	284.26	J (i, ii, iii)
Glycitin	IMPHY008537	-7.5	His79, Asn80, Ser110, Phe113, Tyr114	C ₂₂ H ₂₂ O ₁₀	446.4	K (i, ii, iii)
N6 Methylgmatine	IMPHY005789	-3.8	Gly227, Gly257, Thr264	C ₆ H ₁₆ N ₄	144.22	L (i, ii, iii)

(i)
(D)



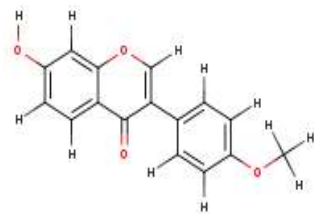
(ii)



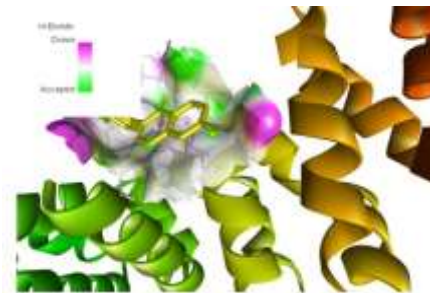
(iii)



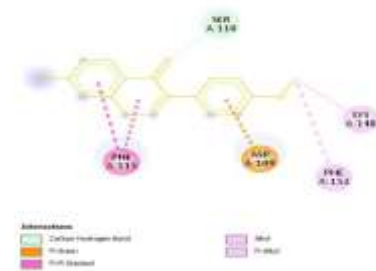
(i)
(E)



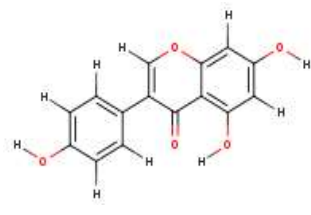
(ii)



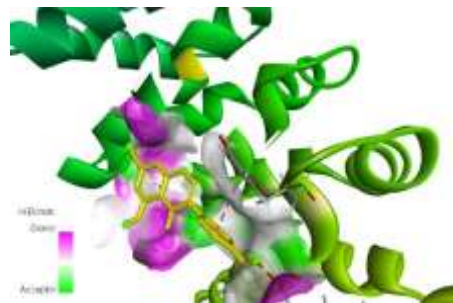
(iii)



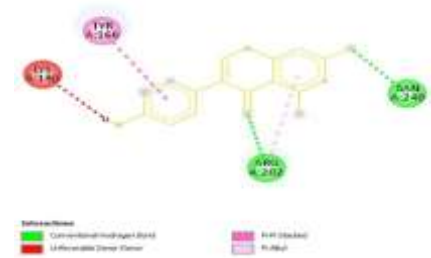
(i)
(F)



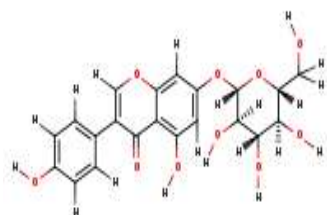
(ii)



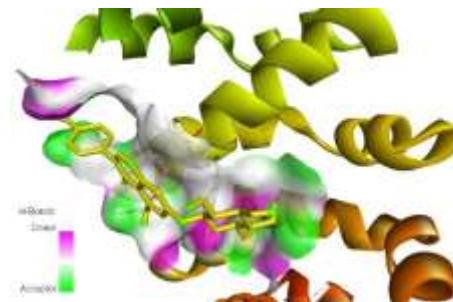
(iii)



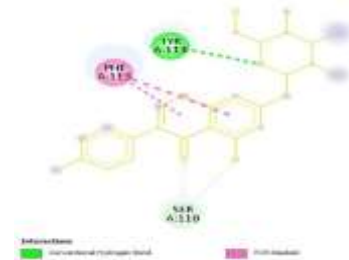
(i)
(G)



(ii)



(iii)



(i)
(H)



(ii)



(iii)



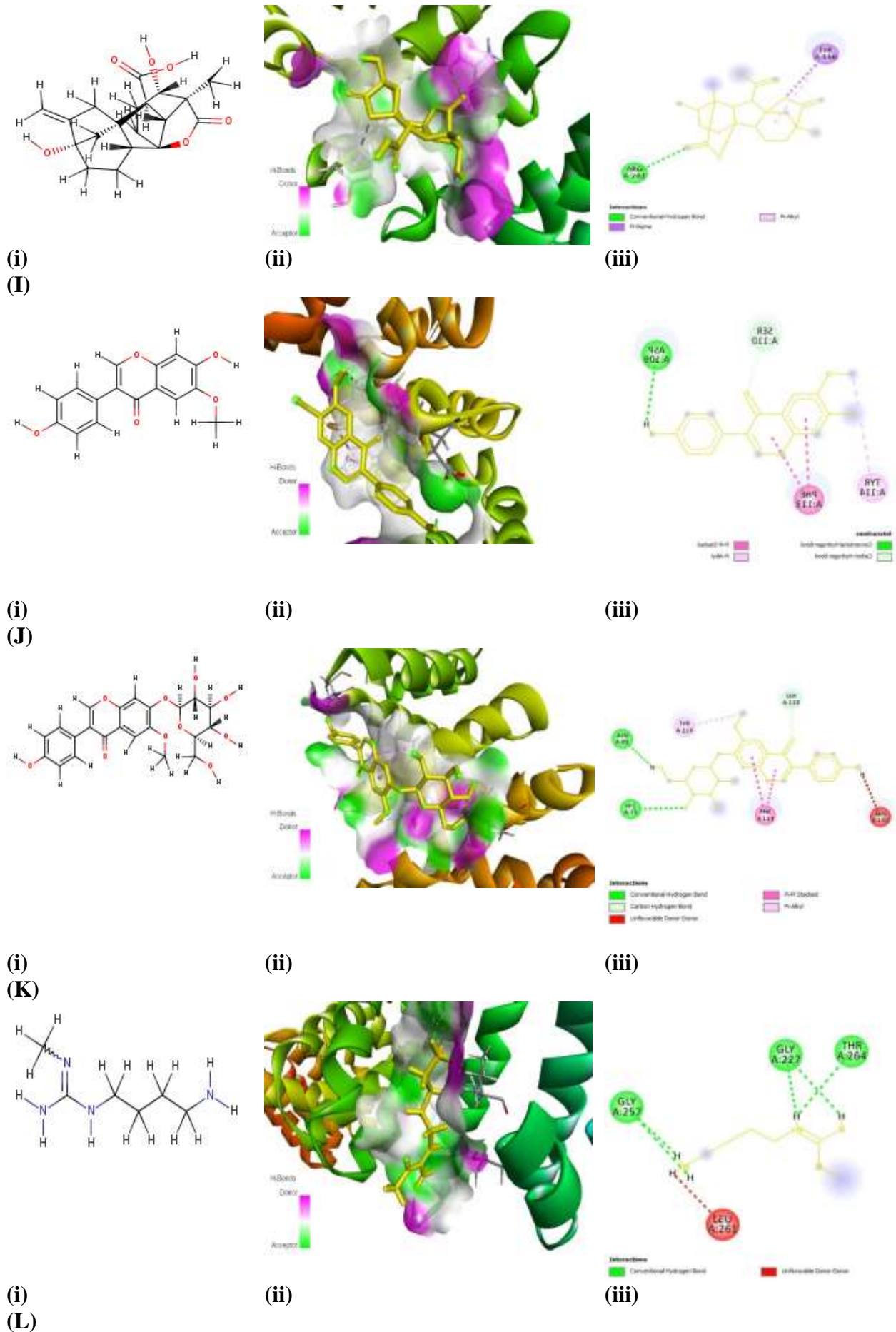


Figure 4(i) Molecular structures of selected ligands, (ii) Molecular docking complexes of ligand with targeted proteins and (iii) 2D view of hydrogen and hydrophobic bond interaction between ligands and target proteins

Where: Ala: Alanine, Arg: Arginine, Asn: Asparagine, Asp: Aspartic acid; Cys: Cysteine; Glu: Glutamic acid, Gln: Glutamine; Gly: Glycine, His: Histidine; Ile: Isoleucine. Leu: Leucine; Lys: Lysine; Met: Methionine; Phe: Phenylalanine; Pro: Proline; Ser: Serine; Thr: Threonine; Trp: Tryptophan; Tyr: Tyrosine; Val: Valine.

Number of heavy metals ranging from 10 to 32 with aromatic heavy atoms numbers from 0-16, while fraction Csp range of 0.00 to 0.83. The number of rotatable bonds present in the selected compounds ranges minimum 0 to maximum 5 and number of hydrogen bond acceptor range from 1 to 10 whereas number of hydrogen bond donor range from 0 to 6. The molar refractivity values starts minimum from 42.9 to maximum 110.5 with TPSA range from 13.14 to 170.05 (Table 4).

Lipophilicity is a key property in transport processes, including intestinal absorption, membrane permeability, protein binding, and distribution to different tissues and organs, including the brain. Lipophilicity is one of the key properties of a potential drug that determines the solubility, the ability to penetrate through cell barriers, and transport to the molecular target. It affects pharmacokinetic processes such as adsorption, distribution, metabolism, excretion (ADME). In this respect, absorption is faster in lipophilic drugs, whereas the ease for renal excretion is greater in hydrophilic medications. Lipophilic properties of selected compounds reveal that iLog P (pan assay interference) ranges from -0.31 to 2.49, the XLog P (the octanol-water partition coefficient) value ranges from -1.64 to 3.66. The WLog P (the water partition coefficient) ranges from minimum -1.41 to maximum 3.17 where as MLogP (Moriguchi Octanol-water partition coefficient) values fall between the range of -2.6 to 1.76. (N-Octanol/water partition) Log Po/w (SILICOS-IT) range varies between -1.15 to 3.52 and consensus LogPo/w ranges minimum -1.42 to maximum 2.83 (Table 5).

The Log S (logarithm of molar solubility in water) indicates the range from -3.878 to 0.288. The E.SOL (estimated solubility) represented in mg/ml ranges between minimum of 1.08 to maximum of 7.63 and in mol/l its range is from 1.06 to 8.89. All these compounds are moderate to highly soluble in water (Table 6).

Pharmacokinetic property of selected compounds reveals that all of them are low to highly absorbable from GIT. Two of them can cross blood brain barrier while the remaining cannot cross BBB. Two of them are P-glycoprotein substrates while the others are not. Half of them inhibits Cytochrome P450 CYP1A2 and CYP2D6 family, none of the inhibits CYP2C19 and CYP2C9 family. Five of the selected compounds inhibit CYP3A4 family while others do not. Regarding their skin permeation (Log Kp) measured in cm/s the range varies from -8.33 to -4.54 (Table 7).

The drug likeliness of all the selected compounds shows that all of them follow Lipinski Rule of 5 with no violation except one with just 1 violation. Two of the do not follow Ghose while rest of the other follow it. Three of them do not follow Veber and Eggans rule with 1 violation each while remaining do follow it. Mugges' rule is followed by seven of the while five of the compounds don't follow it with 1 or 2 violations where molecular weight (MW) is less than 200 and Topological Polar Surface Area (TPSA) of more than 150. The Bioavailability score achieved by all the compounds ranges from 0.55 to 0.56 (Table 8).

Medicinal chemistry of all the selected compounds reveals that all of them do not alter the Pan Assay Interference (PAINS) number except 1 of them while four of them alter Brenk number > Lead Likelihood is shown by half i.e., six of them and synthetic accessibility is achieved in the range minimum of 2.32 to maximum of 5.96 (Table 9).

Table 4 Physicochemical Properties of selected phyto compounds

Phyto compounds	Heavy atoms	Aromatic Heavy atoms	Fraction of Csp3	Rotatable bonds	H-bond acceptors	H-bond donors	Molar Refractivity	TPSA (Å ²)
-----------------	-------------	----------------------	------------------	-----------------	------------------	---------------	--------------------	------------------------

2 Pentylfuran	10	5	0.56	4	1	0	42.9	13.14
Ascorbic acid	12	0	0.5	2	6	4	35.12	107.22
Quercetin	22	16	0	1	7	5	78.04	131.36
Coumesterol	20	17	0	0	5	2	73.81	83.81
Daidzein	30	16	0.29	4	9	5	104.09	149.82
Formononetin	20	16	0.06	2	4	1	76.44	59.67
Genistein	20	16	0	1	5	3	73.99	90.9
Genistin Isoflavones	31	16	0.29	4	10	6	106.11	170.05
Gibberellin A1	25	0	0.79	1	6	3	87.34	104.06
Glycitein	21	16	0.06	2	5	2	78.46	79.9
Glycitin	32	16	0.32	5	10	5	110.58	159.05
N6 Methylagmatine	10	0	0.83	5	2	3	42.86	76.43

Table 5 Lipophilic properties of selected phyto compounds

Phyto compounds	Log Po/w (iLogP)	Log Po/w (XLogP3)	Log Po/w (WLogP)	Log Po/w (MLogP)	Log Po/w (SILICOS-IT)	Consensus Log Po/w
3 pentylfuran	2.63	3.66	3.01	1.84	3.01	2.83
Ascorbic acid	-0.31	-1.64	-1.41	-2.6	-1.15	-1.42
Quercetin	1.63	1.54	1.99	-0.56	1.54	1.23
Coumesterol	1.8	2.76	3.1	1.76	2.88	2.46
Daidzin	2.42	0.67	0.34	-1.11	0.82	0.63
Formononetin	2.49	2.8	3.17	1.33	3.52	2.66
Genistein	1.91	2.67	2.58	0.52	2.52	2.04
Genistin Isoflavones	2.44	0.86	0.05	-1.61	0.35	0.42
Gibberellin A2	1.74	0.23	1.25	1.75	1.72	1.34
Glycitein	2.36	2.44	2.88	0.77	3.03	2.3
Glycitin Blank	2.29	0.64	0.35	-1.39	0.89	0.56
N6 Methylagmatine	1.03	-1.08	-0.74	-0.05	-0.41	-0.25

Table 6 Water Solubility of selected phyto compounds

Phyto compounds	Log S (ESOL)	ESOL Solubility (mg/mL)	ESOL Solubility (mol/L)	ESOL Class	Log S (Ali)	Ali Solubility (mg/mL)	Ali Solubility (mol/L)	Ali Class	Log S (SILICOS-IT)	Silicos-IT Solubility (mg/mL)	Silicos-IT Solubility (mol/L)	Silicos-IT class
3 pentylfuran	-3.11	1.08E-01	7.79E-04	Soluble	-3.63	3.28E-02	2.37E-04	Soluble	-3.59	3.57E-02	2.58E-04	Soluble
Ascorbic acid	0.23	3.01E+02	1.71E+00	Highly soluble	-0.1	1.40E+02	7.93E-01	Very soluble	1.49	5.46E+03	3.10E+01	Soluble
Quercetin-	-3.16	2.11E-01	6.98E-04	Soluble	-3.91	3.74E-02	1.24E-04	Soluble	-3.24	1.73E-01	5.73E-04	Soluble
Coum.represesterol	3.87	3.61E-02	1.35E-04	Soluble	-4.18	1.79E-02	6.68E-05	Moderately soluble	-5.03	2.51E-03	9.38E-06	Moderately soluble
Daidzin	-2.97	4.42E-01	1.06E-03	Soluble	-3.39	1.69E-01	4.05E-04	Soluble	-3.28	2.18E-01	5.22E-04	Soluble
Formononetin	-3.73	5.03E-02	1.87E-04	Soluble	-3.71	5.23E-02	1.95E-04	Soluble	-5.68	5.58E-04	2.08E-06	Moderately soluble
Genistein	-3.72	5.11E-02	1.89E-04	Soluble	-4.23	1.59E-02	5.88E-05	Moderately soluble	-4.4	1.07E-02	3.94E-05	Moderately soluble
Genistin Isoflavones	-3.18	2.85E-01	6.60E-04	Soluble	-4.01	4.18E-02	9.67E-05	Moderately soluble	-2.69	8.77E-01	2.03E-03	Soluble
Gibberellin A2	-2.08	2.91E+00	8.34E-03	Soluble	-1.98	3.69E+00	1.06E-02	Very soluble	-1.93	4.09E+00	1.17E-02	Soluble
Glycitein	-3.57	7.63E-02	2.68E-04	Soluble	-3.76	4.93E-02	1.73E-04	Soluble	-5.1	2.25E-03	7.91E-06	Moderately soluble
Glycitin Blank	-3.05	3.79E-01	8.89E-04	Soluble	-3.56	1.24E-01	2.78E-04	Soluble	-3.38	1.85E-01	4.15E-04	Soluble
N6 Methylagmatine	0.28	2.72E+02	1.89E+00	Highly soluble	-0.04	1.33E+02	9.21E-01	Very soluble	-1.29	7.40E+00	5.13E-02	Soluble

Table 7 Pharmacokinetics of selected phyto compounds

Phyto compounds	GI absorption	BBB permeant	P-gp substrate	CYP1A2 inhibitor	CYP2C19 inhibitor	CYP2C9 inhibitor	CYP2D6 inhibitor	CYP3A4 inhibitor	Log Kp (skin permeation) (cm/s)
3 pentylfuran	High	Yes	No	Yes	No	No	Yes	No	-4.54
Ascorbic acid	High	No	No	No	No	No	No	No	-8.54
Quercetin-	High	No	No	Yes	No	No	Yes	Yes	-7.05
Coumesterol	High	No	No	Yes	No	No	Yes	No	-5.98
Daidzin	Low	No	No	No	No	No	No	No	-8.36
Formononetin	High	Yes	No	Yes	No	No	Yes	Yes	-5.95
Genistein	High	No	No	Yes	No	No	Yes	Yes	-6.05
Genistin Isoflavones	Low	No	Yes	No	No	No	No	No	-8.33
Gibberellin A2	High	No	Yes	No	No	No	No	No	-8.26
Glycitein	High	No	No	Yes	No	No	Yes	Yes	-6.3

Glycitin	Low	No	No	No	No	No	No	Yes	-8.57
N6 Methylagmatine	High	No	-7.95						

Table 8 Drug likeness of selected phyto compounds

Phyto compounds	Lipinski	Ghose	Veber	Egan	Muegge	Bioavailability Score
2 Pentylfuran	Yes; 0 violation	No; 1 violation: MW<160	Yes	Yes	No; 2 violations: MW<200, Heteroatoms<2	0.55
Ascorbic acid	Yes; 0 violation	No; 2 violations: WLOGP<-0.4, MR<40	Yes	Yes	No; 1 violation: MW<200	0.56
Quercetin-	Yes; 0 violation	Yes	Yes	Yes	Yes	0.55
Coumesterol	Yes; 0 violation	Yes	Yes	Yes	Yes	0.55
Daidzin	Yes; 0 violation	Yes	No; 1 violation: TPSA>140	No; 1 violation: TPSA>131.6	Yes	0.55
Formononetin	Yes; 0 violation	Yes	Yes	Yes	Yes	0.55
Genistein	Yes; 0 violation	Yes	Yes	Yes	Yes	0.55
Genistin Isoflavones	Yes; 1 violation: NHorOH>5	Yes	No; 1 violation: TPSA>140	No; 1 violation: TPSA>131.6	No; 2 violations: TPSA>150, H-don>5	0.55
Gibberellin A2	Yes; 0 violation	Yes	Yes	Yes	Yes	0.56
Glycitein	Yes; 0 violation	Yes	Yes	Yes	Yes	0.55
Glycitin	Yes; 0 violation	Yes	No; 1 violation: TPSA>140	No; 1 violation: TPSA>131.6	No; 1 violation: TPSA>150	0.55
N6 Methylagmatine	Yes; 0 violation	No; 2 violations: MW<160, WLOGP<-0.4	Yes	Yes	No; 1 violation: MW<200	0.55

Table 9 Medicinal chemistry of selected phyto compounds

Phyto compounds	PAINS Num. Alters	Brenk Num. Alters	Lead likeness	Synthetic accessibility
3 pentylfuran	0	0	No; 2 violations: MW<250, XLOGP3>3.5	2.32
Ascorbic acid	0	0	No; 1 violation: MW<250	3.47
Quercetin-	1	1	Yes	3.23
Coumesterol	0	1	Yes	3.16
Daidzin	0	0	No; 1 violation: MW>350	5.01
Formononetin	0	0	Yes	2.81
Genistein	0	0	Yes	2.87
Genistin Isoflavones	0	0	No; 1 violation: MW>350	5.12
Gibberellin A2	0	1 alert: isolated_alkene	Yes	5.96
Glycitein	0	0	Yes	2.95
Glycitin	0	0	No; 1 violation: MW>350	5.2
N6 Methylagmatine	0	2 alerts: imine_1, imine_2	No; 1 violation: MW<250	2.33

Where **PAINS**: Pan Assay Interference Compounds, **XLogP**: Octanol-Water Partition Coefficient; **MLogP**: Moriguchi octanol-water partition coefficient; **WLogP**: water partition coefficient, **CYP3**: Cytochrome P450, family 3; **CYP2**: Cytochrome P450, family 2; **CYP1**: Cytochrome P450, family 1; **MW**: molecular weight, **BBB**: Blood Brain barrier, **P-gp**: P-glycoprotein; **LogS**: logarithm of the molar solubility in water, **Log Po/w**: n-octanol/water partition coefficient; **K_p**: skin permeation coefficient, **TPSA**: topological polar surface area; **ESOL**: Estimated SOLubility, **g/mol**: molar mass; **A°**: Angstrom¹⁰-10

3. Molecular Dynamics Simulation

The peaks of RMSF graph represent the fluctuation portion of the protein through the simulation. The N- and C-terminal show more changes than any other portion of the protein. Alpha helices and beta strands show less fluctuation, as they are stiffer than the unstructured part of protein, than loop portion. All protein frames are first aligned on the reference frame backbone, and then the RMSD is calculated based on the atom selection. Monitoring the RMSD of the protein can give insights into its structural conformation throughout the simulation. The RMSD of -complex showed consistency from

almost 4 to 5 Å till 45 ns after that there was a small deviation from 45 to almost 60 ns and then the simulation was converged and stable till 100 ns (Figure 5).

After looking the trajectories, it was found that the both systems were stable and ligands remained inside the binding pockets and made important interactions and the backbones were consistent. Similarly, estimated RMSF values less than 3 Å indicated high stability of the complex and there was fluctuation from 2.4 to almost 4.8. There was no huge fluctuation where ligand made interaction with the receptor showed in green lines (Figure 6).

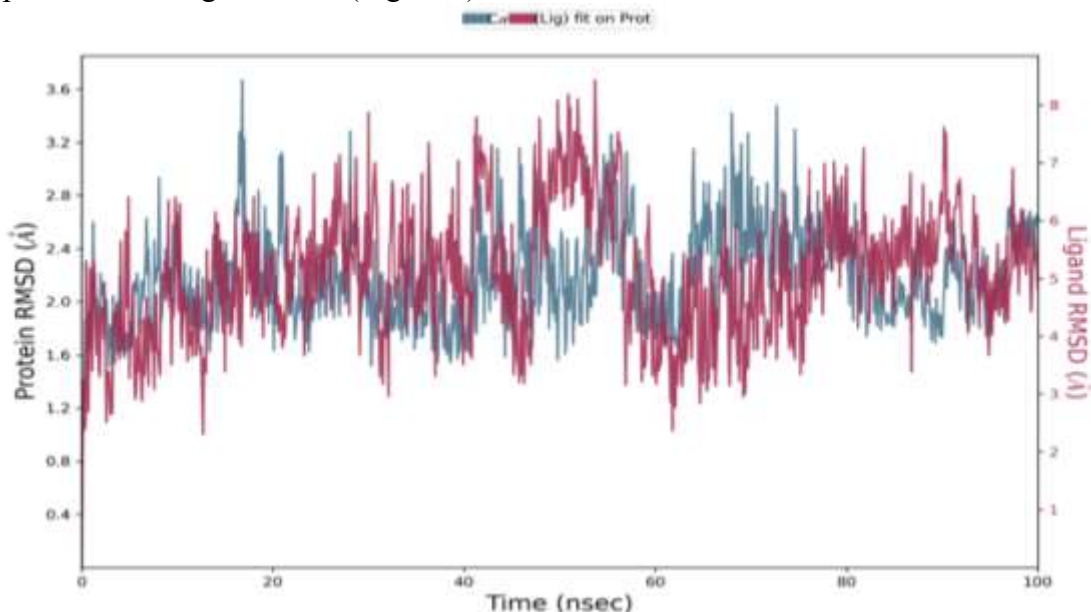


Figure 5Root Mean Square Deviation (RMSD) plot of Disentanglement –Complex

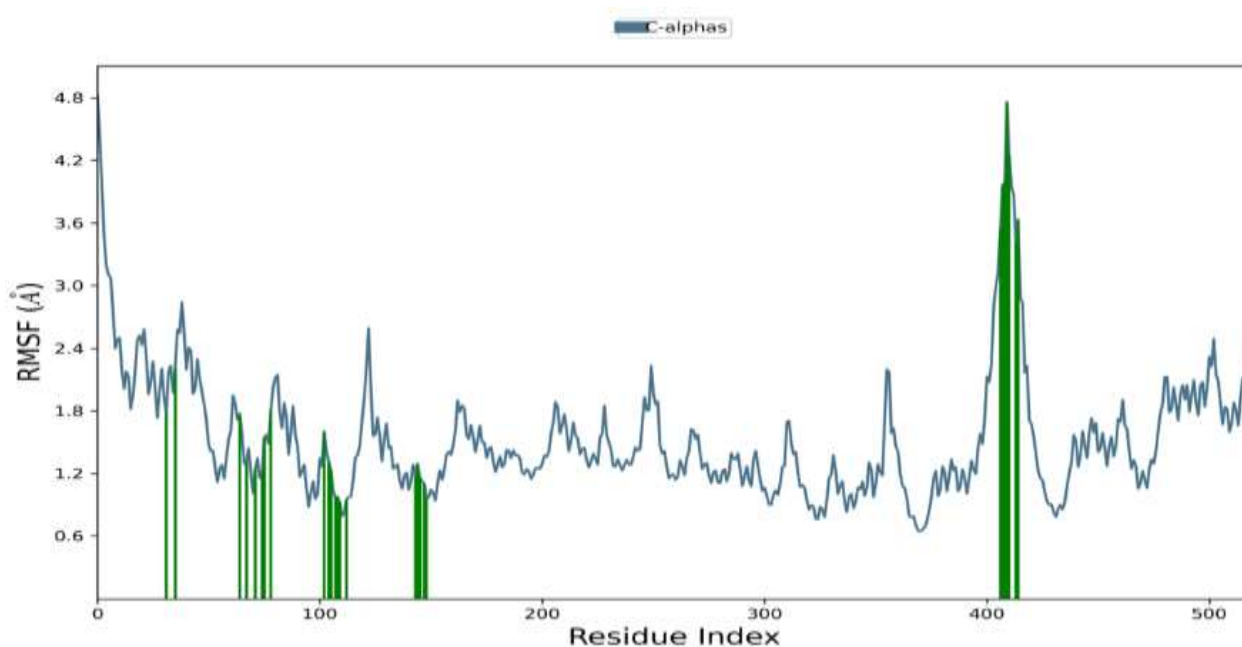


Figure 6Root Mean Square Fluctuation (RMSF) plot of Disentanglement -Complex

The ligand in Disentangle-complex was studied in order to find out the influence of the ligand on over all protein. Six properties were examined to illustrate the stabilities of the selected ligands in the binding pocket during the simulation of 100 ns (1) Ligand RMSD: Root mean square deviation of a ligand with respect to the reference conformation (typically the first frame is used as the reference and it is regarded as time $t = 0$); (2) Radius of gyration (rGyr): It is used to measure the ‘extendedness’

of a ligand, and is equivalent to its principal moment of inertia; (3) intramolecular hydrogen bond (intraHB): Number of internal hydrogen bonds (HB) within a ligand molecule. (4) Molecular surface area (MolSA): Molecular surface was calculated with 1.4 Å probe radius; (5) Solvent accessible surface area (SASA): Molecular surface area of accessible by a water molecule; (6) Polar surface area (PSA): Solvent accessible surface area in a molecule contributed only by oxygen and nitrogen atoms (Figure 7).

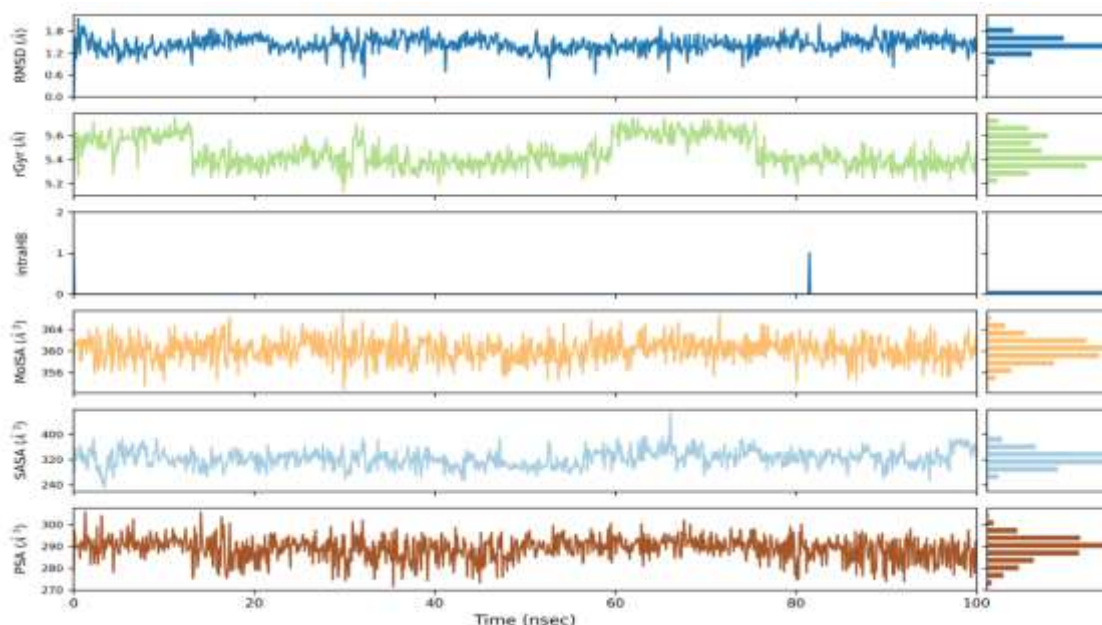


Figure 7 Variation in the ligand's properties in Disentanglement-Complex with respect to time during the course of 100 ns simulation

As shown in figure 8 the RMSD of the ligand was nearly 1.5 Å and it was stabilized at till 100 ns. The rGyr value of ligand in the binding was 5.6 Å till 15 ns and then it was at 5.4 till almost 60 ns after that it was again at 5.6 till almost 75 ns and then it was stabilized at 5.4 till the end of simulation. The MolSA was at 360 Å² throughout the simulation. The SASA and PSA were at 320 and 290 Å² respectively throughout the end of simulation of 100 ns. In the MolSA, SASA and PSA plots for the ligand, there was no much fluctuations observed and they were consistent throughout the simulation.

DISCUSSION

The main reason for the poor survival rate of ovarian cancer patients is due to the lack of screening methods at the early stages and the lack of effective treatments for advanced stages of the disease. Despite of all this variability, mostly advanced staged EOCs are treated with a standard combination of surgery and platinum-based chemotherapy like cisplatin or carboplatin, with taxane like paclitaxel or docetaxel but unfortunately most of the patients develop either resistance or relapse to these therapies (20-23).

Although most patients respond favorably to primary therapy but approximately 75% of advanced EOC patients recur within 3 years of diagnosis and remain incurable unfortunately (24). Hence more efficacious new therapeutic strategies for advanced disease are urgently needed. The standard chemotherapy for EOC patients is a combination of a platinum product, such as cisplatin or carboplatin, with a taxane, such as paclitaxel or docetaxel [3]. However, many patients develop resistance to these therapies and relapse. Recent research has introduced several therapeutic agents that target specific cancer-driven factors to inhibit ovarian cancer development. For example, bevacizumab, an antibody against vascular endothelial growth factor (VEGF)- A, has been approved by the FDA to be used in combination with carboplatin and paclitaxel. Moreover, several Poly (ADP-

Ribose) Polymerase (PARP) inhibitors have been approved for the treatment of recurrent BRCA-mutated EOC

Soy products have been widely consumed in several Asian countries and are served as various kinds of food, such as tempeh, tofu, soymilk, miso, soy nuts, and many more (Messina *et al.*, 2006), which have broad spectrum biological impacts and nutrient values. Multiple phytochemicals of *G. max* L. seed are used as therapeutic agents (Table 10).

Table 10 Functional components of soy and their impact

Phytochemicals of soy	Amount	Biological impacts
Oils out of which ~55% linoleic acid and ~8% α -linolenic acid of total, lecithin, as well as phytosterols, and tocopherols.	19%	Hypotriglyceridemic, Improves heart health
Phospholipids of which ~35% phosphatidyl choline, ~25% phosphatidyl ethanolamine, ~15% phosphatidyl inositol, ~5-10% phosphatidic acid.	1-3%	Structural roles
Non-starch Polysaccharides, oligosaccharides (4% stachyose and 1.1 % raffinose) and Polysaccharides (insoluble dietary fiber)	Variable	Structural roles
Isoflavones and flavonoids(flavones, flavonols, flavanols, aurones, red and blue anthocyanin pigments, and chalcones)	3 mg/g dry weight	Estrogenic, hypocholesterolemic, improves digestive tract function, prevents breast, prostate, and colon cancer, bone health, improve lipid metabolism
Lecithins	-	Improve lipid metabolism, improve memory and learning abilities
Lectins	-	Anti-carcinogenic, immunostimulator
Linoleic acid	-	Hypocholesterolemic
Peptides	-	Readily absorbed, reduce body fat, anticancer
Phytosterols	-	Hypocholesterolemic, improves prostate cancer
Protein (two storage globulins, 11S glycinin and 7S β -conglycinin, hemagglutinin, trypsin inhibitors, α -amylase, lipoxygenases, ferritin)	35–40 %	Hypocholesterolemic, antiatherogenic, reduces body fat
Saponin (triterpene glycosides)	2%	Regulates lipid metabolism, antioxidant
Vitamins (All vitamin except B12 and vitamin C), tocopherols (α , β , γ and δ -tocopherols), thiamine and riboflavin	in trace amount (mg/kg)	Co-enzymes and Co-factors
Minerals (K, P, Ca, Mg, and Fe)	5 %	Transmembrane regulations
Sterols e.g. β -sitosterol (53 to 56%), campesterol (20 to 23%), and stigmasterol (17 to 21%)	300 to 400 mg of sterols per 100 g	Structural roles
Moisture	8.1 gm	Part of cytosole which is site for biochemical reactions
Protein	43.2 gm	Enzymes, structural role
Fat	19.5 gm	Hormones, Enzymes, Transmembrane regulations
Minerals	4.6 gm	Co-enzymes and Co-factors
Crude fiber	3.7 gm	Structural roles
Carbohydrate	20.9 gm	Structural and metabolic roles
Energy	432 Kcal	Metabolic role
Calcium	240 mg	Transmembrane regulations
Phosphorus	690 mg	Transmembrane regulations and Metabolic roles
Iron	10.4 mg	Co-enzymes and Co-factors

Due to the distinct biology of ovarian cancer, the selection of treatment options and effective drug combinations remain limited (4). Therefore, there is an urgent requirement to examine novel and more effective drugs for the treatment of ovarian cancer. Consistently, natural products have shown a diverse range of human health-promoting properties since times immemorial (5). Several studies have reported that the consumption of isoflavonoids is inversely proportional to the risk of cancer (14,15). It has been estimated by Fu *et al.*, (2018) that Daidzein (7,4-dihydroxyisoflavone), a flavone of plant origin, has been reported to exhibit anticancer activity against several types of cancer, including breast and ovarian cancer perhaps due to phytoestrogenic nature. However, the anticancer effect of daidzein has not been thoroughly investigated and the detailed mechanisms remain to be elucidated. Daidzein exerts antiproliferative effects on SKOV3 cells. The antiproliferative effect of daidzein against a panel of human ovarian cancer cells and normal (Moody) ovarian cells was evaluated using a CCK-8 assay. The results indicated that, of all ovarian cancer cell lines, daidzein exerted the most marked dose-dependent antiproliferative effects on SKOV3 cells. However, daidzein was found to be less cytotoxic against the normal cells. The IC_{50} of daidzein against the SKOV3 cells was 20 μ M,

compared with the IC₅₀ of 100 μM for the normal ovarian cells. In addition, daidzein affected the morphology of the SKOV3 cells. As daidzein exhibited the lowest IC₅₀ against SKOV3 cells, subsequent experiments were performed using only this cell line. As the concentration of daidzein was increased, the SKOV3 cancer cells became rounder, shrunken and detached from the substratum, which are important morphological changes associated with apoptosis. Moreover, daidzein triggers mitochondrial apoptosis. As daidzein induced morphological changes in the SKOV3 cells characteristic of apoptosis, DAPI and AO/EB staining were performed. Daidzein also induced apoptosis of the SKOV3 cells, as evident from the increasing number of nuclei stained white in the case of DAPI staining and showing orange fluorescence in the case of AO/EB staining. In addition to daidzein induces G2/M cell cycle arrest. Cell cycle arrest is one of the important mechanisms by which anticancer agents exert their inhibitory effects. Therefore, the present study also determined the effect of daidzein treatment on cell cycle phase dissemination of the SKOV3 cells. The results indicated that the number of SKOV3 cells was significantly enhanced in the G2 phase at doses of 0-40 μM daidzein, leading to G2/M cell cycle phase arrest. Daidzein inhibits cell migration. The present study also examined whether daidzein can inhibit the migration of SKOV3 cancer cells at the different concentrations using a wound-healing assay. The results of the wound-healing assay showed that daidzein reduced the migratory capability of the SKOV3 cells in a dose-dependent manner. In the control group, the cells exhibited the capacity to migrate, whereas treatment led to cells showing reduced potential to migrate. Daidzein inhibits the RAF/MEK/ERK signaling pathway.

The RAF/MEK/ERK signaling pathway has been shown to be important in the tumorigenesis and progression of several types of cancer, including ovarian cancer. Daidzein inhibits tumor growth *in vivo*. SKOV3 tumor growth was significantly suppressed by daidzein administration, compared with that in the control group. At the end of the 4-week period of daidzein treatment, the average tumor growth and volume in the untreated control group were considerably higher than those in the treated groups.

Daidzein has multiple pharmacological effects on vital organs of human body like it is anti-hypertensive and anti-cardiovascular as it reduced platelet aggregation and nitric oxide production and is anti-inflammatory because it increases level of peroxisome proliferator-activated receptors gamma (PPAR γ) and adiponectin. It is neuroprotective as it inhibits glutamate induced apoptosis and neurotoxicity and has anti-alzheimer effects. It also has antiaging effects as it is anti-inflammatory, photo-protective and also interferes with melanin synthesis pathway by inhibiting melanin production. Daidzein is also responsible for antiosteoporosis by maintaining bone density of women specially in post-menopausal conditions. It also reduces the expression of human epidermal growth factor receptor-2 (HER2/neu) and proliferating-cell nuclear antigen thus reduces breast, colon and prostate cancers. It is antidiabetic as it increases in activity of glucose transporter type 4 (GLUT4) transporters through AMP-activated protein kinase activation. It also activates superoxide dismutase (SOD), glutathione peroxidase (GPx) and catalase (CAT) enzymes which eliminates reactive oxygen species (Cortez et al., 2018).

REFERENCES

1. <https://www.cancer.org/cancer/ovarian-cancer/detection-diagnosis-staging/staging.html>
2. Aberrant non-canonical WNT pathway as key-driver of high-grade serous ovarian cancer development Gian Franco Zannoni^{1,2} & Giuseppe Angelico¹ & Angela Santoro¹ Virchows Archiv (2020) 477:321–322
3. <https://doi.org/10.1007/s00428-020-02760-5>, Prat J (2012). Ovarian carcinomas: five distinct diseases with different origins, genetic alterations, and clinicopathological features. Virchows Arch 460(3):237–249. <https://doi.org/10.1007/s00428-012-1203-5>
4. Wnt Signaling in Ovarian Cancer Stemness, EMT, and Therapy Resistance J. Clin. Med. 2019, 8, 1658; doi:10.3390/jcm8101658.
5. [Wnt Signaling in Ovarian Cancer Stemness, EMT, and Therapy Resistance Miriam Teeuwssen * and Riccardo Fodde * J. Clin. Med. 2019, 8, 1658; doi:10.3390/jcm8101658 3

6. Kurman, R.J.; Shih Ie, M. Pathogenesis of ovarian cancer: Lessons from morphology and molecular biology and their clinical implications. *Int. J. Gynecol. Pathol.* 2008, 27, 151–160.]
7. [3Kurman, R.J.; Shih Ie, M. Pathogenesis of ovarian cancer: Lessons from morphology and molecular biology and their clinical implications. *Int. J. Gynecol. Pathol.* 2008, 27, 151–160.]
8. (Wnt Signaling in Ovarian Cancer Stemness, EMT, and Therapy Resistance Miriam Teeuwssen * and Riccardo Fodde *J. Clin. Med.* 2019, 8, 1658; doi:10.3390/jcm8101658)
9. [1: Wnt/ β -catenin signaling in ovarian cancer: Insights into its hyperactivation and function in tumorigenesis Nguyen et al. *Journal of Ovarian Research* (2019) 12:122 <https://doi.org/10.1186/s13048-019-0596->
10. Logan CY, Nusse R. The Wnt signaling pathway in development and disease. *Annu Rev Cell Dev Biol.* 2004;20:781–810.].
11. [1: Clevers H. Wnt/beta-catenin signaling in development and disease. *Cell.* 2006;127(3):469–80, 2: Polakis P. The many ways of Wnt in cancer. *Curr Opin Genet Dev.* 2007; 17(1):45–51.
12. [9 Logan CY, Nusse R. The Wnt signaling pathway in development and disease. *Annu Rev Cell Dev Biol.* 2004;20:781–810.??]
13. (22 Stamos JL, Weis WI. The beta-catenin destruction complex. *Cold Spring Harb Perspect Biol.* 2013;5(1):a007898)
14. (Stamos JL, Weis WI. The beta-catenin destruction complex. *Cold Spring Harb Perspect Biol.* 2013;5(1):a007898.).
15. (Wnt/ β -catenin signalling in ovarian cancer: Insights into its hyperactivation and function in tumorigenesis Vu Hong Loan Nguyen¹, Rebecca Hough¹, Stefanie Bernaudo¹ and Chun Peng Nguyen et al. *Journal of Ovarian Research* (2019) 12:122 <https://doi.org/10.1186/s13048-019-0596-z>)**[27**
16. Ref: Wnt/ β -Catenin Signaling in Development and Disease, Hans Clevers. DOI 10.1016/j.cell.2006.10.018
17. Pharmacologic Manipulation of Wnt Signaling and Cancer Stem Cells Yann Duchartre¹, Yong-Mi Kim¹, Michael Kahn^{2,3} *Methods Mol Biol.* 2017 ; 1613: 463–478. doi:10.1007/978-1-4939-7027-8_18)).
18. ((Phytochemicals: A Multitargeted Approach to Gynecologic Cancer Therapy Lee Farrand,¹ Se-Woong Oh,¹ Yong Sang Song,^{2,3,4} and Benjamin K. Tsang Hindawi Publishing Corporation BioMed Research International Volume 2014, Article ID 890141, 10 page <http://dx.doi.org/10.1155/2014/890141>))
19. {{Opportunity, Challenge and Scope of Natural Products in Medicinal Chemistry, 2011: 367-383 ISBN: 978-81-308-0448-4. Soybean constituents and their functional benefits Ajay K. Dixit¹, J. I. X. Antony¹, Navin K. Sharma¹ and Rakesh K. Tiwari²}}
20. Wnt/ β -catenin signaling in ovarian cancer: Insights into its hyperactivation and function in tumorigenesis Vu Hong Loan Nguyen¹, Rebecca Hough¹, Stefanie Bernaudo¹ and Chun Peng Nguyen et al. *Journal of Ovarian Research* (2019) 12:122 <https://doi.org/10.1186/s13048-019-0596-z>).
21. Cortez AJ, Tudrej P, Kujawa KA, Lisowska KM. Advances in ovarian cancer therapy. *Cancer Chemother Pharmacol.* 2018;81:17–38
22. Luvero D, Milani A, Ledermann JA. Treatment options in recurrent ovarian cancer: latest evidence and clinical potential. *Ther Adv Med Oncol.* 2014; 6(5):229–39
23. Coleman RL, Monk BJ, Sood AK, Herzog TJ. Latest research and treatment of advanced-stage epithelial ovarian cancer. *Nat Rev Clin Oncol.* 2013;10(4): 211–24].
24. [6 Coleman RL, Monk BJ, Sood AK, Herzog TJ. Latest research and treatment of advanced-stage epithelial ovarian cancer. *Nat Rev Clin Oncol.* 2013;10(4): 211–24].
25. Rehman HM, Sajjad M, Ali MA, Gul R, Naveed M, Aslam MS, Shinwari K, Bhinder MA, Ghani MU, Saleem M, Rather MA, Ahmad I, Amin A. Identification of RdRp inhibitors against SARS-CoV-2 through E-pharmacophore-based virtual screening, molecular docking and MD simulations approaches. *Int J Biol Macromol.* 2023 May 15;237:124169. doi:

- 10.1016/j.ijbiomac.2023.124169. Epub 2023 Mar 28. PMID: 36990409; PMCID: PMC10043960.
26. Gul, R., Hanif, M.U., Gul, F. et al. Molecular Cloning, Expression, Sequence Characterization and Structural Insight of Bubalus bubalis Growth Hormone-Receptor. *Mol Biotechnol* (2022). <https://doi.org/10.1007/s12033-022-00612-y>
 27. Rehman HM, Sajjad M, Ali MA, Gul R, Irfan M, Naveed M, Bhinder MA, Ghani MU, Hussain N, Said ASA, Al Haddad AHI, Saleem M. Identification of NS2B-NS3 Protease Inhibitors for Therapeutic Application in ZIKV Infection: A Pharmacophore-Based High-Throughput Virtual Screening and MD Simulations Approaches. *Vaccines*. 2023; 11(1):131. <https://doi.org/10.3390/vaccines11010131>
 28. Shinwari K, Rehman HM, Liu G, Bolkov MA, Tuzankina IA, Chereshev VA. Novel Disease-Associated Missense Single-Nucleotide Polymorphisms Variants Predication by Algorithms Tools and Molecular Dynamics Simulation of Human TCIRG1 Gene Causing Congenital Neutropenia and Osteopetrosis. *Front Mol Biosci*. 2022 Apr 28; 9:879875.
 29. **Asma Ahmed***, Ghazala Irshad, Sania Riaz, Rehana Badar, Sana Javaid Awan, Shafaq, Ambreen Abbas. Polarity based extracts of *Glycine max* (L.) seeds as therapeutic source for ovarian, uterine and hepato-renal profile of sprague dawley rats with letrozole-induced polycystic ovarian syndrome. (2023). *Hunan Daxue Xuebao/Journal of Hunan University Natural Sciences*. ISSN : 1674-2974 | CN 43-1061 / N. 60 (04): 11- 28. DOI 10.17605/OSF.IO/7YHTW
 30. Waris, Ghazala & Ahmed, Asma & Rukhsar, Atoofa & Zahra, Fatima-tu & Malik, Areesha. (2023). FORMONONETIN AS PROMISING THERAPEUTIC INTERVENTION FOR RESTORING OVARIAN, UTERINE, AND HEPATO-RENAL FUNCTIONS IN LETROZOLE-INDUCED, POLYCYSTIC OVARIAN SYNDROME SPRAGUE DAWLEY RATS. *Journal of Population Therapeutics and Clinical Pharmacology*. 727-735. 10.53555/jptcp.v30i19.3749.
 31. **Evaluation of the hypoglycemic activity of *Morchella conica* by targeting protein tyrosine phosphatase 1B.** Naema Begum, Abdul Nasir, Zahida Parveen*, Taj Muhammad, **Asma Ahmed**, Saira Farman, Nargis Jamila, Mohib Shah, Noor Shad Bibi, Akif Khurshid, Zille Huma, Atif Ali Khan Khalil, Ashraf Albrakati and Gaber El-Saber Batiha. *Frontiers in Pharmacology (Ethnopharmacology)*. 2021. 12; 1-12. DOI: 10.3389/fphar.2021.661803.
 32. **Isolation, Purification and Quantification of Quercetin from Onion (*Allium cepa* L.).** **Asma Ahmed**, Muhammad Gulfraz, Noman Khalique. *Proceedings of Pakistan Academy of Sciences*. Vol. 55 (1), March 2018. Page: 79- 86; ISSN 0377-2969.
 33. Wu, J., Zhou, T., Wang, Y., Jiang, Y., & Wang, Y. (2021). Mechanisms and Advances in Anti-Ovarian Cancer with Natural Plants Component. *Molecules (Basel, Switzerland)*, 26(19), 5949. <https://doi.org/10.3390/molecules26195949>
 34. Zhang, J., Liu, L., Wang, J., Ren, B., Zhang, L., & Li, W. (2018). Formononetin, an isoflavone from *Astragalus membranaceus* inhibits proliferation and metastasis of ovarian cancer cells. *Journal of ethnopharmacology*, 221, 91–99. <https://doi.org/10.1016/j.jep.2018.04.014>
 35. Farah Naz Tahir, **Asma Ahmed***, Aisha Riaz, Samra Hafeez, Shaista Javaid. Effects of polarity-based extracts of partially oxidized *Camellia sinensis* L. leaves on lipid profile of streptozotocin induced hyperlipidemic albino Wistar rats. *Hunan Daxue Xuebao/Journal of Hunan University Natural Sciences*. ISSN : 1674-2974 | CN 43-1061 / N. 60 (04): 11- 28. DOI 10.17605/OSF.IO/7YHTW
 36. Hasan Akbar Khan, **Asma Ahmed***, Khadija Kiran, Samra Hafeez, Rehana Badar, Sajjad Ahmad. (2023). Phyto compound-based drug discovery approach to explore the frostbite healing potential of Abietadiene isolated from *Pinus roxburghii*. *Journal of Population Therapeutics & Clinical Pharmacology*. Vol. 30 (17): 1968-1986. DOI: 10.53555/jptcp.v30i17.2900
 37. Jing Zhang, Likun Liu, Jing Wang, Baoyin Ren, Lin Zhang, Weiling Li. Formononetin, an isoflavone from *Astragalus membranaceus* inhibits proliferation and metastasis of ovarian cancer

- cells. *Journal of Ethnopharmacology*. Volume 221. 2018. Pages 91-99. ISSN 0378-8741. <https://doi.org/10.1016/j.jep.2018.04.014>
38. Ferreira, P. S., Victorelli, F. D., Fonseca-Santos, B., & Chorilli, M. (2019). A Review of Analytical Methods for p-Coumaric Acid in Plant-Based Products, Beverages, and Biological Matrices. *Critical reviews in analytical chemistry*, 49(1), 21–31. <https://doi.org/10.1080/10408347.2018.1459173>
39. Pandi, A., & Kalappan, V. M. (2021). Pharmacological and therapeutic applications of Sinapic acid-an updated review. *Molecular biology reports*, 48(4), 3733–3745. <https://doi.org/10.1007/s11033-021-06367-0>
40. Fogacci F, Tocci G, Presta V, Fratter A, Borghi C, Cicero AF (January 2018). "Effect of resveratrol on blood pressure: A systematic review and meta-analysis of randomized, controlled, clinical trials". *Critical Reviews in Food Science and Nutrition*. 58 (2): 1605–1618. doi:10.1080/10408398.2017.1422480
41. Cooney, Christopher R.; Varley, Zoë K.; Nouri, Lara O.; Moody, Christopher J. A.; Jardine, Michael D.; Thomas, Gavin H. (2019-04-16). "Sexual selection predicts the rate and direction of colour divergence in a large avian radiation". *Nature Communications*. 10 (1): 1773. Bibcode:2019NatCo..10.1773C. doi:10.1038/s41467-019-09859-7. ISSN 2041-1773. PMC 6467902. PMID 30992444.
42. Kim, Sin-Yeon; Velando, Alberto (January 2020). "Attractive male sticklebacks carry more oxidative DNA damage in the soma and germline". *Journal of Evolutionary Biology*. 33 (1): 121–126. doi:10.1111/jeb.13552. ISSN 1420-9101. PMID 31610052. S2CID 204702365.
43. Timlin, Jerilyn A.; Collins, Aaron M.; Beechem, Thomas A.; Shumskaya, Maria; Wurtzel, Eleanore T. (2021), "Localizing and Quantifying Carotenoids in Intact Cells and Tissues", *Carotenoids*, InTech, doi:10.5772/68101, ISBN 978-953-51-3211-0, S2CID 54807067.
44. Powers, Matthew J; Hill, Geoffrey E (2021-05-03). "A Review and Assessment of the Shared-Pathway Hypothesis for the Maintenance of Signal Honesty in Red Ketocarotenoid-Based Coloration". *Integrative and Comparative Biology*. 61 (5): 1811–1826.
45. Khadija Gilani, **Asma Ahmed**, Rehana Badar, Shaista Javaid, Mehmood ul Hassan, Shagufta Naz, Sami Ullah. (2023). Global Metabolomics Analysis of Pakistani Citrus Cultivars Infected with Huanglongbing or Citrus Greening. *International Journal of Phytopathology*. Vol. 12 (2): 161-185. DOI: 10.33687/phytopath.012.02.4620
46. Tatli Cankaya, I. I., & Somuncuoglu, E. I. (2021). Potential and Prophylactic Use of Plants Containing Saponin-Type Compounds as Antibiofilm Agents against Respiratory Tract Infections. *Evidence-based complementary and alternative medicine : eCAM*, 2021, 6814215. <https://doi.org/10.1155/2021/6814215>
47. Li, X., Xin, Y., Mo, Y., Marozik, P., He, T., & Guo, H. (2022). The Bioavailability and Biological Activities of Phytosterols as Modulators of Cholesterol Metabolism. *Molecules (Basel, Switzerland)*, 27(2), 523. <https://doi.org/10.3390/molecules27020523>
48. Chen TC, Da Fonseca CO, Schönthal AH (2015). "Preclinical development and clinical use of perillyl alcohol for chemoprevention and cancer therapy". *American Journal of Cancer Research*. 5 (5): 1580–93. PMC 4497427. PMID 26175929
49. Zhang, Yuan; Li, Xing; Ciric, Bogoljub; Curtis, Mark T.; Chen, Wan-Jun; Rostami, Abdolmohamad; Zhang, Guang-Xian (6 April 2020). "A dual effect of ursolic acid to the treatment of multiple sclerosis through both immunomodulation and direct remyelination". *Proceedings of the National Academy of Sciences*. 117 (16): 9082–9093. doi:10.1073/pnas.2000208117
50. Cargnin ST, Gnoatto SB (April 2017). "Ursolic acid from apple pomace and traditional plants: A valuable triterpenoid with functional properties". *Food Chem*. 220: 477–489.
51. Forman, V., Luo, D., Geu-Flores, F. *et al*. A gene cluster in *Ginkgo biloba* encodes unique multifunctional cytochrome P450s that initiate ginkgolide biosynthesis. *Nat Commun* 13, 5143 (2022). <https://doi.org/10.1038/s41467-022-32879-9>

52. Palliyaguru, D. L., Yuan, J. M., Kensler, T. W., & Fahey, J. W. (2018). Isothiocyanates: Translating the Power of Plants to People. *Molecular nutrition & food research*, 62(18), e1700965. <https://doi.org/10.1002/mnfr.201700965>
53. Asif Ali, M., Khan, N., Kaleem, N., Ahmad, W., Alharethi, S. H., Alharbi, B., Alhassan, H. H., Al-Enazi, M. M., Razis, A. F. A., Modu, B., Calina, D., & Sharifi-Rad, J. (2023). Anticancer properties of sulforaphane: current insights at the molecular level. *Frontiers in oncology*, 13, 1168321. <https://doi.org/10.3389/fonc.2023.1168321>
54. Ansari, M. I., Khan, M. M., Saquib, M., Khatoon, S., & Hussain, M. K. (2018). Dithiolethiones: a privileged pharmacophore for anticancer therapy and chemoprevention. *Future medicinal chemistry*, 10(10), 1241–1260. <https://doi.org/10.4155/fmc-2017-0281>
55. Zhang, Y., & Munday, R. (2008). Dithiolethiones for cancer chemoprevention: where do we stand?. *Molecular cancer therapeutics*, 7(11), 3470–3479. <https://doi.org/10.1158/1535-7163.MCT-08-0625>
56. Yudhistira, B., Punthi, F., Lin, J. A., Sulaimana, A. S., Chang, C. K., & Hsieh, C. W. (2022). S-Allyl cysteine in garlic (*Allium sativum*): Formation, biofunction, and resistance to food processing for value-added product development. *Comprehensive reviews in food science and food safety*, 21(3), 2665–2687. <https://doi.org/10.1111/1541-4337.12937>
57. Kundu, A.; Quirit, J. G.; Khouri, M. G.; Firestone, G. L. (2017). "Inhibition of oncogenic BRAF activity by indole-3-carbinol disrupts microphthalmia-associated transcription factor expression and arrests melanoma cell proliferation". *Molecular Carcinogenesis*. 56 (1): 49–61. doi:10.1002/mc.22472
58. Arumugam, M. K., Paal, M. C., Donohue, T. M., Jr, Ganesan, M., Osna, N. A., & Kharbanda, K. K. (2021). Beneficial Effects of Betaine: A Comprehensive Review. *Biology*, 10(6), 456. <https://doi.org/10.3390/biology10060456>
59. FU HUA, CHANG-HUA LI, XIAO-GANG CHEN and XIAO-PING LIU. **Daidzein exerts anticancer activity towards SKOV3 human ovarian cancer cells by inducing apoptosis and cell cycle arrest, and inhibiting the Raf/MEK/ERK cascade.** 2018. DOI: 10.3892/ijmm.2018.3531).